Postfach 10 11 61
69451 Weinheim
Germany
Courier services:
Boschstraße 12
69469 Weinheim
Germany
Tel.: (+49) 6201 606 235
Fax: (+49) 6201 606 500
E-mail: advhealthmat@wiley-vch.de

WILEY-VCH

Dear Author,

Please correct your galley proofs carefully and return them no more than three days after the page proofs have been received.

If you have not used the PXE system before, please view the Tutorial before checking your proofs: http://wileypxe.aptaracorp.com/pxewileyvch/UserDocument/UserGuide/WileyPXE5_AuthorInstructions.pdf

Please note any queries that require your attention. These are indicated with red Qs in the pdf or highlighted as yellow queries in the "Edit" window.

Please pay particular close attention to the following, as no further corrections can be made once the article is published online:

- **Names** of all authors present and spelled correctly
- **Titles** of authors are correct (Prof. or Dr. only: please note, Prof. Dr. is not used in the journals)
- **Addresses of all authors** and **e-mail address of the corresponding author** are correct and up-to-date
- **Funding bodies** have been included and grant numbers are accurate
- The **Title** of the article is OK
- All **figures** are correctly included
- **Equations** are typeset correctly

Note that figure resolution in the PXE system is deliberately lower to reduce loading times. This will be optimized before the article is published online.

Please send any additional information, such as figures or other display items, to advhealthmat@wiley-vch.de, and please also indicate this clearly in the PXE "Edit" window by inserting a comment using the query tool.

Reprints may be ordered by filling out the accompanying form.
Return the reprint order form by e-mail with the corrected proofs, to Wiley- VCH: **advhealthmat@wiley-vch.de**

Please limit corrections to errors already in the text. Costs incurred for any further changes will be charged to the author, unless such changes have been agreed upon by the editor.

The editors reserve the right to publish your article without your corrections if the proofs do not arrive in time. Note that the author is liable for damages arising from incorrect statements, including misprints.

ADVANCED HEALTHCARE MATERIALS

Reprint Order Form 2017
- please return with your proofs -

Editorial Office:

Wiley-VCH Verlag, Boschstrasse 12
69469 Weinheim, Germany

Tel.: (+49) 6201 606 235
Fax: (+49) 6201 606 500

E-mail: advhealthmat@wiley-vch.de
http://www.advhealthmat.de

Manuscript No. _____

Please send me and bill me for

☐ no. of **reprints** via ☐ airmail (+ 25 Euro) ☐ surface mail

☐ **high-resolution PDF file** (330 Euro).

My e-mail address:

_____

Please note: It is not permitted to present the PDF file on the internet or on company homepages

★**Special Offer**★ If you order 200 or more reprints you will get a PDF file for half price.

Information regarding VAT
Please note that from German sales tax point of view, the charge for **Reprints, Issues or Posters** is considered as **"supply of goods"** and therefore, in general, such delivery is a subject to German sales tax. However,this regulation has no impact on customers located outside of the European Union. Deliveries to customers outside the Community are automatically tax-exempt. Deliveries within the Community to institutional customers outside of Germany are exempted from the German tax (VAT) only if the customer provides the supplier with his/her VAT number. The VAT number (value added tax identification number) is a tax registration number used in the countries of the European Union to identify corporate entities doing business there. It starts with a country code (e.g. FR for France, GB for Great Britain) and follows by numbers.

Cover Posters

Posters are available of all the published covers and frontispieces in two sizes

☐ DIN A2 42 x 60 cm/ 17 x 24in (one copy: **39 Euro**)

☐ DIN A1 60 x 84 cm/ 24 x 33in (one copy: **49 Euro**)

Postage for shipping posters overseas by airmail:
+ 25 Euro

Postage for shipping posters within Europe by surface mail:
+ 15 Euro

Mail reprints / cover posters to:

_____
_____
_____
_____
_____

Invoice address:

_____
_____
_____
_____
_____

_____
Date, Signature **Stamp**

VAT no.: _____
(institutes / companies in EU countries only)

Purchase Order No.: _____

Credit Card Payment

VISA, MasterCard, AMERICAN EXPRESS
Please use the Credit Card Token Generator located at the website below to create a token for secure payment. The token will be used instead of your credit card number.

Credit Card Token Generator:
https://www.wiley-vch.de/editorial_production/index.php

Please transfer your token number to the space below.

Credit Card Token Number:

Price list for reprints (The prices include mailing and handling charges. All Wiley-VCH prices are exclusive of VAT)

No. of pages	Price (in Euro) for orders of 50 copies	100 copies	150 copies	200 copies	300 copies	500 copies
1-4	345	395	425	445	548	752
5-8	490	573	608	636	784	1077
9-12	640	739	786	824	1016	1396
13-16	780	900	958	1004	1237	1701
17-20	930	1070	1138	1196	1489	2022
for every additional 4 pages	147	169	175	188	231	315

★ **Special Offer** ★ If you order 200 or more reprints you will get a PDF file for half price.

Wiley-VCH Verlag GmbH & Co. KGaA; Location of the Company: Weinheim;
Chairman of the Supervisory Board: Stephen Michael Smith,
Trade Register: Mannheim, HRB 432833, General Partner: John Wiley & Sons GmbH,
Location: Weinheim, Trade Register Mannheim, HRB 432296,
Managing Director: Sabine Steinbach

WILEY-VCH

Communication

xxxx

M. Giannaccini, M. P. Calatayud, A. Poggetti, S. Corbianco, M. Novelli, M. Paoli, P. Battistini, M. Castagna, L. Dente, P. Parchi, M. Lisanti, G. Cavallini, C. Junquera, G. F. Goya, V. Raffa* .....x–xx

Magnetic Nanoparticles for Efficient Delivery of Growth Factors: Stimulation of Peripheral Nerve Regeneration

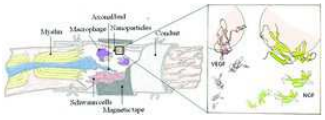

Magnetic nanoparticles (MNPs) carrying the nerve growth factor and the vascular growth factor are localized in the center of a nerve guidance conduit sutured between two nerve stumps after nerve axotomy. MNP-mediated delivery enhances the regeneration process and the recovery of motor function, whereas the delivery of free factors, which have a short half-life, has no effects.

adhm201601429(201601429)

Materials Views
www.MaterialsViews.com

ADVANCED HEALTHCARE MATERIALS
www.advhealthmat.de

Magnetic Nanoparticles for Efficient Delivery of Growth Factors: Stimulation of Peripheral Nerve Regeneration

*Martina Giannaccini, M. Pilar Calatayud, Andrea Poggetti, Silvia Corbianco, Michela Novelli, Melania Paoli, Pietro Battistini, Maura Castagna, Luciana Dente, Paolo Parchi, Michele Lisanti, Gabriella Cavallini, Concepción Junquera, Gerardo F. Goya, and Vittoria Raffa**

ABSTRACT: The only clinically approved alternative to autografts for treating large peripheral nerve injuries is the use of synthetic nerve guidance conduits (NGCs), which provide physical guidance to the regenerating stump and limit scar tissue infiltration at the injury site. Several lines of evidence suggest that a potential future strategy is to combine NGCs with cellular or molecular therapies to deliver growth factors that sustain the regeneration process. However, growth factors are expensive and have a very short half-life; thus, the combination approach has not been successful. In the present paper, we proposed the immobilization of growth factors (GFs) on magnetic nanoparticles (MNPs) for the time- and space-controlled release of GFs inside the NGC. We tested the particles in a rat model of a peripheral nerve lesion. Our results revealed that the injection of a cocktail of MNPs functionalized with nerve growth factor (NGF) and with vascular growth factor (VEGF) strongly accelerate the regeneration process and the recovery of motor function compared to that obtained using the free factors. Additionally, we found that injecting MNPs in the NGC is safe and does not impair the regeneration process, and the MNPs remain in the conduit for weeks.

Q1

The use of nerve guidance conduits (NGCs) is the only clinically approved alternative to autograft for the treatment of large peripheral nerve injuries. NGCs provide a conduit during the nerve regeneration process for the diffusion of growth factors secreted by the injured nerve ends and limit injury site infiltration by scar tissue.[1] Current knowledge suggests that NGCs should be combined with the delivery of molecules[2] such as guidance cues (e.g., netrins, ephrins, semaphorins, and other molecules capable of orientating migrating and growing cells) and factors that influence neuronal growth (e.g., growth factors, neurotransmitters, and extracellular matrix proteins).[3] Among tested molecules, nerve growth factor (NGF) was shown to have a stimulatory effect on fiber growth.[4] The administration of exogenous NGF significantly improves the recovery of neurological function after peripheral nerve injury.[5,6] However, a phase 3 trial for diabetic neuropathy and a phase 2 trial for HIV-related neuropathy failed to demonstrate any substantial effect of NGF treatment. These negative results have been ascribed to the poor bioavailability of NGF due to its short half-life (2–5 min).[7] This finding has stimulated much research on the use of alternative modes of delivery.[6,8,9] Similarly, it is well recognized that vascular growth factor (VEGF) stimulates peripheral nerve regeneration due to its angiogenic potential and neurotrophic potential,[10,11] but its short in vivo half-life (approximately half an hour[12]) also limits the effectiveness of VEGF as a therapeutic agent, which could explain the conflicting results regarding the real benefit of VEGF administration

Q6

Dr. M. Giannaccini, Prof. L. Dente, Prof. V. Raffa, Department of Biology, Università di Pisa, S.S. 12 Abetone e Brennero 4, 56127 Pisa, Italy

Q2

Dr. M. P. Calatayud, Prof. G. F. Goya, Instituto de Nanociencia de Aragon, Universidad de Zaragoza, Mariano Esquillor 50018 Zaragoza, Spain

A. Poggetti, Dr. S. Corbianco, Dr. M. Novelli, P. Battistini, Prof. M. Castagna, Dr. P. Parchi, Prof. M. Lisanti, Dr. G. Cavallini, Department of Translational Research and of New Surgical and Medical Technologies, Università di Pisa, Via Savi 8 56126, Pisa, Italy

M. Paoli, Prof. V. Raffa, Institute of Life Science, Scuola Superiore Sant'Anna, Piazza Martiri della Libertà 33, 56127 Pisa, Italy

Prof. C. Junquera, Institute for Health Research Aragon IIS, Fac Med, C Domingo Miral S-N, Zaragoza 50009, Spain

Q3

Q5

Correspondence to: Prof. V. Raffa (E-mail: vittoria.raffa@unipi.it)

10.1002/adhm.201601429

for functional recovery after nerve injury.[13] Similar considerations apply to the administration of other neurotrophic factors, such as brain-derived neurotrophic factor and glial cell-derived neurotrophic factor (GDNF).[14] In vitro studies have shown that conjugation to iron oxide magnetic nanoparticles (MNPs) can strongly prolong the activity of several growth factors, such as NGF, GDNF, and basic fibroblast growth factor (FGF-2).[15,16] An additional advantage of MNPs is that they can be remotely guided by magnetic fields. This guidance could provide an extraordinary advantage because during the normal physiological regeneration process, cells infiltrate, proliferate, and migrate from both ends of the damaged nerve toward the center, and the concentration of the secreted factors, which are responsible for the regeneration process, is inversely proportional to the distance from the center. The magnetic properties of MNPs could thus be advantageously exploited to localize the functionalized particles to the center of the conduit where the concentration of factors and cell localization is usually minimal. In the present study, we validated a drug delivery approach mediated by MNPs to obtain the maximum effect of exogenous growth factors. Specifically, we produced a neurotmesis of the rat median nerve with two nerve stumps that were sutured to the ends of a synthetic conduit filled with the particles (Figure S1, Supporting Information). We demonstrated that the MNPs do not trigger any adverse side effects, even at a dose 350-fold higher than the working dose. Injection and localization of 0.9 μg of MNPs carrying 100 ng of NGF and 29 ng of MNPs carrying 5.6 ng of VEGF in the center of the conduit strongly improved nerve regeneration and the recovery of motor function, whereas the same amount of free factors had no effects. Similarly, poor or no effects have been reported in literature by using drug delivery systems carrying similar amounts of NGF[17] or VEGF[18] without control of growth factor localization.

Following the transection of the nerve, the section distal to the injury site degenerated, and the tissue ultrastructure was compromised. Specifically, the ultrastructure of the injured nerve showed complete axonal degeneration (**Figure 1**A1), blood extravasation, and destruction of the myelin sheath (Figure 1B1). Many phagocytic cells invaded the area and cleared the degenerated myelin and cellular debris (Figure 1C1). Functional recovery was then totally dependent on the reconstruction of the ultrastructure of a healthy nerve (Figure S2, Supporting Information). Axons must grow and extend from the proximal end across the injured site until they reach their distal target.[19] The regenerative process within a silicone tube across a rat sciatic nerve gap has been already described,[20,21] and we observed the same regeneration steps in our model. Our experiments were designed to determine particle localization over weeks and whether the presence of the particles would trigger any unwanted side effects or impair the spontaneous regeneration process. Our experimental evidence indicated that even a high dose (33 μg) of MNPs did not interfere with the regeneration process: nerve regeneration proceeded spontaneously at a certain rate without differences between the groups injected with MNPs or saline. We found that, 5 d after surgery, the conduit was filled by a matrix consisting of longitudinal fibrin strands, erythrocytes, cellular debris, and extracellular fluids. This fibrin matrix was progressively infiltrated by cells emigrating from both ends of the transected stumps toward the center of the conduit (Figure S3, Supporting Information). In the MNP group, many particles were localized within the matrix (Figure S3, Supporting Information). One week after surgery, the most prevalent type of cells engulfing the particles was macrophages. MNPs were localized within primary endosomes (Figure 1A2), endolysosomes (Figure 1B2) and heterolysosomes, which contained MNPs and a lipid drop (Figure 1C2). The particles were also localized to cells that formed junctions with neighboring cells that were not macrophages (Figure 1D2,E2). Some MNPs were also found in the cell cytoplasm (Figure 1E2). Transmission electron microscopy (TEM) analysis of the ultrastructure clearly showed that the extent of progression of the regeneration process was the same in both groups. Many macrophages and phagocytic cells were actively digesting degenerated myelin (Figure 1C1,H2 for saline and MNP groups, respectively). Many mesenchymal cells were present (contributing to the reconstruction of the connective tissue by secreting collagen and facilitating the process of damage repair), and many activated fibroblasts with a dilated rough endoplasmic reticulum (ER) (for manufacturing more proteins necessary to rebuild the structure or to sustain axonal growth) were observed (Figure 1D1,E1 and F2,G2 for saline and MNP groups, respectively). Figure 1,I2,J2 shows a Schwann cell (SC) that wrapped four axons (the initial step to actuate the remyelination process).

During the second week of repair, this fibrin cable provided a rail for SCs, fibroblasts, and endothelial cells that migrated from both the proximal and distal nerve stumps (cellular phase). These cells subsequently proliferated and aligned to form a biological tissue cable that replaced the fibrin cable (which was almost degraded) and provided a trophic and topographical route for the axonal phase of repair.[22] Accordingly, in both groups, we found that SCs invaded the matrix, proliferated and aligned to the tissue cable (Figure S4, Supporting Information), and the regenerating axons, which used this biological cable tissue as a guidance mechanism, appeared to reach their distal target (Figure S4, Supporting Information). In the MNP group, the particles were localized in the entire explant, i.e., in both the healthy ends and the regenerating tissue. Similar localization was observed 3 weeks after surgery, with particles inside the regenerating tissue (Figure S4, Supporting Information). TEM confirmed that the particles were still abundant in the tissue in the third week (**Figure 2**A, arrows). Many particles were still found inside macrophages (Figure 2B), but most of the particles were found inside SCs. Figure 2D,E shows MNPs inside a phagocytic cell that is digesting MNPs and myelin and is most likely an SC. Similarly, Figure 2F shows MNPs in an SC (a phagocytic cell with a large and elongated nucleus). In general, MNPs were present around the area of regenerating axons (Figure 2C) but were rarely found in the neuronal processes (they can bind to axons but are not inside the axons). Again, this observation reflects the stage of the regeneration process in which SCs play a prominent role and provide both trophic and topographical routes for axonal repair. In the third week, we observed a massive alignment of SCs with the fibrin cable (Figure S4, Supporting Information)

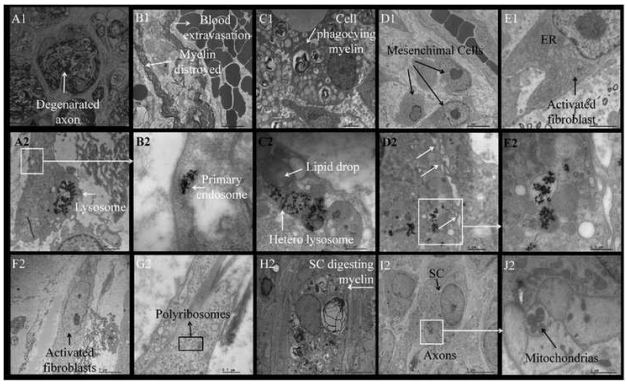

Figure 1. TEM ultrastructure of ultrathin sections of the regenerating tissue 1 week after surgery. A1–E1) Conduit injected with saline. A2–J2) Conduit injected with MNPs. A1) Degenerated axon. B1) Blood extravasation and myelin degeneration. C1) Cells phagocytosing electron-dense whorls of degenerated myelin. D1) Mesenchymal-like cells. E1) Fibroblasts with dilated rough ER. A2) MNPs inside a lysosome. B2) Magnification of the rectangle in panel (A) showing MNPs within a primary endosome. C2) MNPs inside a heterolysosome (a lysosome fused to an electron-lucent fat vacuole). D2,E2) Progressively increasing magnification showing MNPs inside a cell connected to neighboring cells. F2,G2) Fibroblast cytoplasm containing excess free polyribosomes. H2) Schwann cell containing electron-dense whorls of degenerated myelin. I2,J2) Remyelination process by a Schwann cell wrapping four axons. The myelin sheath of the axons under repair was not yet formed at this stage.

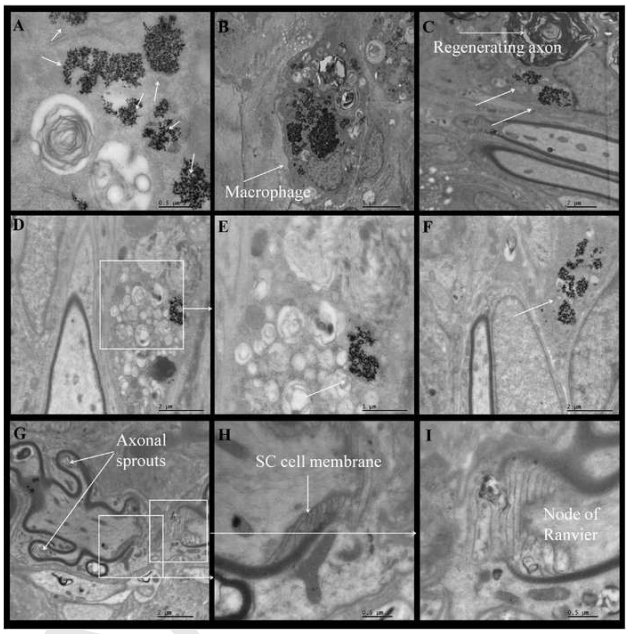

Figure 2. TEM ultrastructures of ultrathin sections of regenerating tissue 3 weeks after surgery. Sample injected with MNPs. A) The arrows point to large aggregates of MNPs. B) A macrophage that has engulfed MNPs and degenerated myelin. C) MNPs localized close to regenerating axons. D,E) A cell containing MNPs and digesting degenerated myelin. F) MNPs near a Schwann cell. Regenerated axons, with evidence of G) axonal sprouts, H) axonal remyelination, and I) a node of Ranvier.

in the two groups. The tissue showed many signs of the repair process, and there were no morphological differences between the two groups (MNPs and saline). Many SCs wrapped axons and actuated the remyelination process. Figure 2G–I shows the regenerated axons with new axonal sprouts (Figure 2G), which started the remyelination phase (Figure 2H). The general structure appeared to correspond to a good stage of reconstruction, as exemplified by the visualization of nodes of Ranvier in some cases (Figure 2I). Additionally, remyelination proceeded at the same rate in both samples (Figure S4, Supporting Information).

Our observations indicate that the particles likely do not trigger any inflammatory processes and do not interfere with the physiological regeneration process. Additionally, the histological examination of the sample injected with MNPs did not reveal any increment in the population of resident phagocytic cells at this time point with respect to the control, and the macrophages appeared to be present in similar amounts in the two groups.

Next, we explored the use of MNPs for the delivery of NGF and VEGF. NGF has been encapsulated in delivery systems previously.[23] When loaded on polymeric microspheres immobilized in an NGC (an acellular allograft prepared from a sciatic nerve) with fibrin glue, NGF (dose of ≈150 ng per conduit) increased the axon number, diameter, and myelin thickness at the 2nd week after nerve repair, but there was no functional recovery of muscle tension between the NGF-microsphere-treated group and the acellular graft at the 16th week after surgery.[8] Interestingly, VEGF was also found to improve peripheral nerve regeneration after axotomy, although the molecular mechanisms underlying that improvement are not completely clear.[10] The authors tested conduits filled with Matrigel supplemented with 500–700 ng mL^{-1} VEGF. This work seemed to suggest that the effects could be indirect (i.e., the increased vascularization sustained axonal regeneration and SC migration). In fact, there was no significant improvement compared with the control (plain Matrigel) in the total area of axonal and SC staining in the conduit inner region at 10 and 15 d after surgery, whereas a statistically significant difference was observed at time points of 30 d or later. In this work, we validated an approach based on the incorporation of NGF and VEGF in MNPs injected in the conduit and demonstrated for the first time that very small amounts of factors, i.e., 100 ng of NGF (concentration in the conduit, 12.5 μg mL^{-1}) and 5.6 ng of VEGF (700 ng mL^{-1}) improves nerve regeneration in the short term (documented by histological analysis) and medium term (documented by motor function assessment). Briefly, we functionalized the particles with factors to reach a concentration of 195 μg of protein per mg of MNP for MNP-VEGF (**Figure 3**A1) and 110 μg of protein per mg of MNP for MNP-NGF (Figure 3A2). MNP-NGF was validated in a PC12 cell line, confirming the ability to induce a neuron-like phenotype (Figure 3A3, particle characterization described in Figure S5, Sup-

porting Information). Validation of MNP-VEGF in a zebrafish model of neoangiogenesis induction confirmed the ability of MNP-VEGF to carry the proangiogenic stimulus (Figure 3A4, particle characterization described in Figure S5, Supporting Information). In this study, we took advantage of the magnetic properties of the particles to localize the growth factors in the center of the conduit (Video of the Supporting Information), where the pattern of axonal and SC staining is usually at a minimum.[10] We analyzed the tissue morphology 12 d after surgery (previous studies using similar amounts of NGF or VEGF did not find morphological improvements at this time point[4,10]). The study was performed on six rats with the right forelimb as the control side (conduit injected with free NGF and VEGF, hereafter labeled the GF group) and the left forelimb as the treatment side (conduit injected with MNP-NGF and MNP-VEGF, hereafter labeled the MNP-GF group). Both sides received the same amount of growth factors, i.e., 100 ng of NGF (12.5 μg mL^{-1}) and 5.6 ng of VEGF (700 ng mL^{-1}). The total amount of MNPs injected in the left arm was 929 ng. Twelve days after surgery, the regenerating nerves were explanted. In three rats (50% incidence), we observed extreme tissue thinning on the right side (GF group), which resulted in tissue discontinuity during tissue processing for histology (i.e., a break between the distal and the proximal ends was observed in the tissue sections). By contrast, in all six rats (100% incidence), continuous tissue was macroscopically observed in the explants from the left side (MNP-GF group), with the distal and proximal ends well interconnected by structured tissue in the lumen. In the three rats with no tissue discontinuity on both the left and right sides, we evaluated the histology of the tissue in the middle of the conduit. The left and right explants were very different macroscopically (Figure 3B1,B2). The regenerating segment of the explants treated with the free growth factors was rich in amorphous material (Figure 3B2), whereas the explants treated with the functionalized particles had structured matter throughout the entire length (Figure 3B1). Most importantly, the tissue treated with MNP-GFs contained an outgrowth of regenerated axons connecting the proximal and distal nerve stumps. Specifically, the sections were covered by neurofilaments (brown staining, Figure 3C1), and analysis of the content of the longitudinal sections revealed the strong presence of SCs in the central position of the tube lumen (brown staining, Figure 3D1) as well. By contrast, immunostaining for NF and S100 was low in any sample treated with the same amount of GFs (Figure 3C2,D2). Panel (E) of Figure 3 provides a quantitative analysis, expressed as the fold increase in the stained area of tissues treated with MNP-GFs versus free GFs ($n = 3$, each value is the mean of four sections). Specifically, we observed a 3.5-fold increase in the NF200-positive area and a twofold increase in the S100-positive area of the MNP-GF group versus the free GF group. Collectively, these findings showed that the regeneration process proceeded faster after MNP-mediated delivery of the growth factors.

The recovery of motor function in the rats was also assessed during the study period at 2, 4, and 6 weeks using the grasping test. The ratio of the grip force to animal weight was used to compare the "MNP-GFs" group with the "GFs" sham group. Preoperatively, the normalized mean force was similar for the

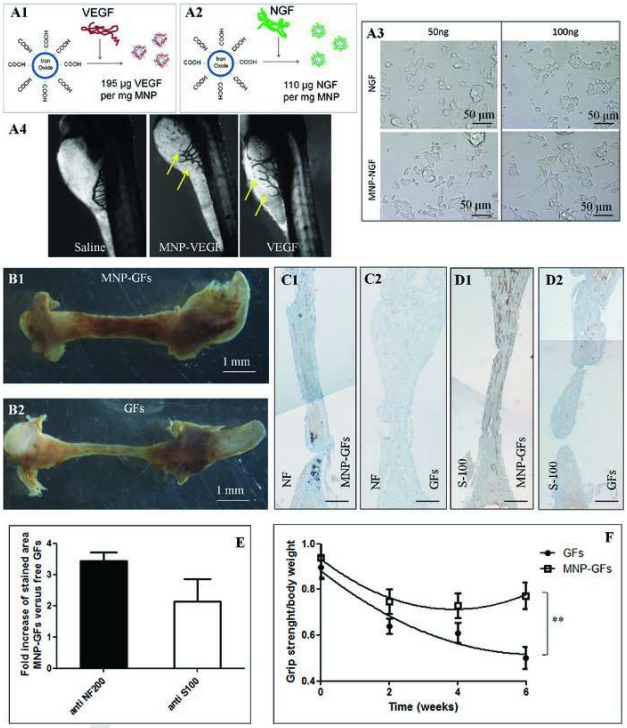

Figure 3. A1) Synthesis of MNP-VEGF. A2) Synthesis of MNP-NGF. A3) PC12 cells differentiated upon incubation with MNP-NGF, similarly to control cells (treated with the same amount of free NGF). A4) The subintestinal vein (SIV) region at 48 h post-fertilization (hpf) in zebrafish embryos: the pattern of blood vessels is clearly defined, with precise networks that were easily stained with alkaline phosphatase. The proangiogenic stimulus from VEGF or MNP-VEGF resulted in a change in the phenotype, with alterations in the basket architecture (supernumerary vessels and irregular formation, yellow arrows). Treatment with VEGF or MNP-VEGF induced the same angiogenic phenotype, whereas treatment with saline resulted in the wild-type phenotype. B1) Explant of the tissue treated with MNP-GFs 12 d after surgery. B2) Explant of the tissue treated with GFs 12 d after surgery. C) NF staining of a longitudinal section of the entire regenerating nerve, which was injected with C1) MNP-GFs or C2) GFs alone. D) S100 staining of a longitudinal section of the entire regenerating nerve injected with D1) MNP-GFs or D2) GFs alone 12 d after surgery. Top: Proximal end. Bottom: Distal end. The scale bar in (C) and (D) is 200 μm. E) Data analysis of the stained area ($n = 3$). F) Grip strength normalized to the animal body weight over time for the MNP-GFs group and the sham group (GFs). Two-way ANOVA followed by Bonferroni correction. **indicates significance at $p < 0.01$.

two groups, i.e., 0.94 ± 0.08 and 0.90 ± 0.05 for the MNP-GFs and GFs groups, respectively. After surgery, all rats showed functional deficits and substantial loss of function. However, two weeks after surgery, the functional deficit was less pronounced in the MNP-GFs group (0.75 ± 0.05) than in the GFs group (0.64 ± 0.03), and this difference increased at the fourth week after surgery (0.73 ± 0.05 for the MNP-GFs group and

0.61 ± 0.04 for the GFs group). In general, the curves corresponding to the MNP-GFs and GFs groups were significantly different ($p = 0.03$), with the control group showing a progressive loss of motor function from the beginning until the end of the study, in sharp contrast to the MNP-GFs group, which exhibited a clear improvement in motor function by the sixth week. Indeed, a significant improvement in function was observed at the sixth week in the MNP-GFs treated group (0.77 ± 0.06) compared with the GFs group (0.50 ± 0.05) ($p < 0.01$) (Figure 3F).

Improvement of functional recovery is the ultimate and most important goal of studies of peripheral nerve repair. In this study, the MNP-treated animals exhibited improved functional performance, in agreement with the histological observations. The increase in neurofilaments and SCs at an early stage of the regeneration process (10 d after surgery) and the enhanced grasp force 6 weeks after injury were indicative of improved reinnervation.

MNPs are a powerful tool to protect growth factors from rapid degradation, as documented by comparative stability studies of free versus conjugated factors.[16] In particular, the NGF conjugated to MNPs was significantly more stable in medium or under tissue culture conditions, with a 100% increase in the residual amount after 3 d of incubation. Incubation of free NGF and MNP-NGF in protease-enriched serum was reported to result in complete degradation of free NGF by day seven, whereas no significant change from the initial concentration was observed for MNP-NGF throughout the seven days.[24] In fact, we previously demonstrated that the MNP-NGF complex is stable in cell culture medium conditions, indicating that nonspecific adsorption of medium proteins does not alter the stability and the integrity of the conjugate.[25] Different mechanisms contribute to the release of GF, such as the rate of dissolution of the MNP polymer shell in the extracellular matrix or, following cell internalization, endosome-mediated hydrolysis, enzymolysis, and redox processes occurring in the cytosol.[26] Interestingly, MNPs can be used to improve both the stability of factors over time and their localization in space. During the physiological repair of a nerve injury, the growth factors that sustain the regeneration process are endogenously secreted by cells that migrate from the proximal and distal stumps of the lesion toward the center. Cell localization in the conduit is not uniform, and thus the concentration of factors along the gap is nonuniform. This is exemplified by histogram A in **Figure 4**, which plots the typical profile of anti-S100 staining (which is representative of the localization of SC, the main source of factors during spontaneous regeneration) along the conduit. The concentration rapidly decreases from the two stumps, reaching quasi 0 values in the center of the conduit. These changes in concentration partially explain the importance of gap length in successful injury recovery and the failure to repair lesions larger than 3–4 cm in humans and 15 mm in rodents via the use of conduits.[1] Histogram B in Figure 4 plots the typical profile of MNP concentration in the conduit, which reaches a maximum in the center and rapidly decreases approaching the ends. Indeed, in this work, we used the magnetic properties of MNPs to provide an exogenous source of growth factor to compensate for the endogenous concentration profile. Another advantage of MNPs is their contribution in maintaining factors in situ. In fact, in addition to loss due to instability, the loss of exogenously administered factors over time is due to physiological tissue washing, which naturally occurs in vivo.

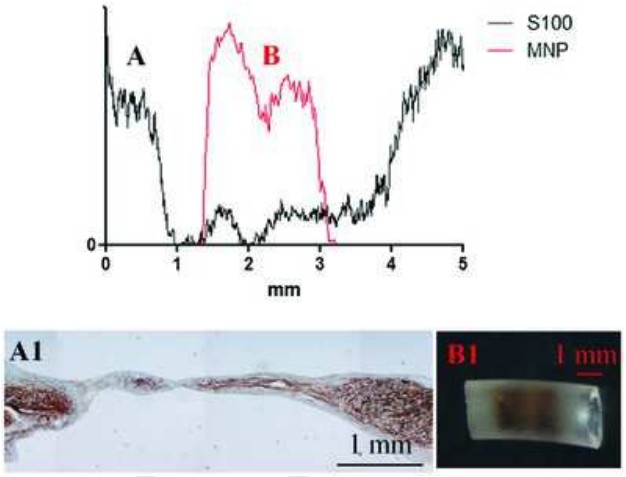

Figure 4. A) Plot profile of anti-S100 staining 10 d postsurgery. B) Plot profile of MNP concentration in the magnetic tape-coated conduit (33 μg of MNPs in the conduit).

In conclusion, we postulate that the increase in stability and the local change in growth factor concentration mediated by MNPs are responsible for the enhanced neuroprotective effects of VEGF and NGF in the MNP group compared with the sham group. The magnetic properties of MNPs can be advantageously exploited to increase GF stability and to localize the functionalized MNPs to the center of the conduit where the concentration of cells and endogenous factors usually reaches the minimum level. Here we demonstrate that this nanotechnology-based approach could improve levels of regeneration and functional recovery of existing NGCs and it could be considered as a realistic alternative to autografts, which have been the gold standard along the last 50 years.

Experimental Section

Particles: The particles used in this study were polyethylenimine (PEI)-coated iron oxide nanoparticles, which the authors extensively characterized in several neural in vitro models[25,27–30] and which showed no detectable signs of toxicity. The MNPs were synthesized as previously described.[27] The MNPs had a magnetic iron oxide core (average core size $\langle d \rangle = 25 \pm 5$ nm, saturation magnetization $M_S = 58$ Am^2 kg^{-1} at $T = 300$ K) and a thin polymer PEI coating (0.7–0.9 nm).[27]

Recombinant VEGF produced in bacteria (Figure S5, Supporting Information) and commercially available NGF (Sigma, Louis, MO, USA, N1408) were used. Particles were functionalized with the protein according to a previously published protocol.[25] Briefly, 1 mg of particles was ultracentrifuged (18 000 *g*) and resuspended in 500 μL of water. After 10 min, the

protein was added (the MNP:protein ratio was 3.5:1 w/w and 5:1 w/w for VEGF and NGF, respectively), followed by mixing for 1 h at 4–8 °C. The unbound protein was removed by ultracentrifugation (18 000 *g*) and discarding the supernatant (two washing steps). The nanoparticles were suspended in a 20% aqueous glycerol solution, and 5 μL aliquots were stored at −20 °C. Storage at −20 °C in 20% glycerol prevented protein degradation, protein desorption from the particles, and particle precipitation. Samples were thawed immediately before injection in the conduit. This storage condition assured the stability of the construct for up to 6 months.

The amount of protein bound to the surface of the MNPs was determined via the Bradford protein assay by subtraction, i.e., by measuring the absorbance of the supernatant derived from the washing steps. The protein concentration was determined from a calibration curve obtained using known amounts of protein (Abs = $0.499x + 0.006$, $R^2 = 0.999$, x = protein concentration in mg mL^{-1}) (VERSAmax, Molecular Devices, Sunnyvale, California, USA). The amount of nanoparticles was determined using a thiocyanate assay. Briefly, the particles were dissolved in 1:1 v/v HCl 6 M HNO_3 (65%) for 1 h at 60 °C. Potassium thiocyanate was added to the Fe^{3+} solution, and then the iron concentration was determined by spectrophotometric measurements at 478 nm. The iron concentration was determined by comparing the sample absorbance to a calibration curve (Abs = $0.056x$, $R^2 = 0.9994$, x = MNP concentration in mg mL^{-1}).[31] The composition of MNP-VEGF was 1.8 mg mL^{-1} MNPs, 350 μg mL^{-1} VEGF, and 20% glycerol. The composition of MNP-NGF was 4.5 mg mL^{-1} MNPs, 500 μg mL^{-1} NGF, and 20% glycerol.

MNP-NGF or free NGF was evaluated in PC12 cells (ATCC, Manassas, VA, USA) incubated in serum-reduced media (1% FBS). MNP-VEGF or free VEGF was microinjected into the yolks of anesthetized zebrafish at 24 hpf, and blood vessels of whole embryos were stained using alkaline phosphatase staining (BCIP/NBT Alkaline Phosphatase Substrate Solution, Roche Diagnostic, Mannheim, Germany) (authorization no. 99/2012-A, 19.04.2012). A detailed validation of MNP-NGF and MNP-VEGF bioactivity is provided in Figure S5 (Supporting Information).

Rat Model: Animal studies were performed in Sprague–Dawley rats obtained from a commercial source (Envigo, Udine, IT). For this study, the authors used 28 young adult female rats. The experimental procedures were approved by the local Ethical Committee of the University of Pisa to conform to Italian "Decreto Legislativo 4 marzo 2014 n. 26" (Rettorale no. 0009069/2014 del 20/03/2014). The model the authors used in this work was the rat median nerve, originally described by Bertelli et al.[32] It was a widely used model to study different strategies for nerve reconstruction (with or without a nerve gap), such as terminoterminal and terminolateral neurorrhaphy and both biological and artificial nerve conduits.[33] Surgery was performed under general anesthesia. The right upper limb of the rat was used as a control and the left was used in experiments. On the right side, the authors produced a neurotmesis, followed by removal of 5 mm of nerve, repair with a synthetic conduit (5 mm in length, inner volume 8 μL) consisting in suturation of the two nerve stumps to the conduit with two staples (10/11-0 nylon) and injection of saline into the conduit. A similar procedure was performed on the left side, but MNPs were injected in place of saline (**Figure 5**A). For the cytotoxicity experiments, the animals were injected with 33 μg of MNPs in the left side and the same volume of saline in the right side, and the animals were sacrificed 1, 2, and 3 weeks after surgery ($n = 6$ per time point). For regeneration experiments, the conduit was modified by wrapping the external surface (1.5 mm in the center) with magnetic tape (Supermagnete, Gottmadingen, Germany, MT-20-STIC) to localize the injected particles in the center of the conduit (Video of the Supporting Information). The tape was coated with a thin film of polyacrylamide to prevent tissue-tape interaction (Figure 5B). The animals were injected with a mixture of MNP-NGF (0.9 μg of MNPs carrying 100 ng of NGF) and MNP-VEGF (29 ng of MNPs carrying 5.6 ng of VEGF) into the left side, and the same amount of free growth factors NGF + VEGF was injected into the right side. To do that, the mother solutions were diluted 1:500 for MNP-VEGF (or VEGF) and 1:40 for MNP-NGF (or NGF) in the final volume and 8 μL of this volume was injected in the conduit (the concentration in the conduit of NGF, VEGF, and glycerol was 12.5 μg mL^{-1}, 700 ng mL^{-1}, and 0.54%, respectively, for both groups). The animals were sacrificed 12 d after surgery for histology ($n = 6$) or 6 weeks after surgery for functional studies ($n = 4$). Functional assessment was performed using the grip strength test (preoperatively and 2, 4, and 6 weeks postoperatively). For histology, particles, neurofilaments, SCs, myelin, and cell morphology were stained with a Prussian Blue kit (Sigma, Louis, MO, USA), an anti-NF-200 monoclonal antibody (Thermo Scientific 1:100, Waltham, MA, USA), an anti-S100 monoclonal antibody (Sigma 1:200, Louis, MO, USA), Luxol fast blue, and pararosaniline/toluidine blue, respectively. The stained area was quantified using the software Fiji (ImageJ). Analysis was performed in the inner portion of the conduit (length, 2 mm). The signal from DAB staining was isolated using the command "color deconvolution" (R:0.26814753, G:0.57031375, B:0.77642715). The sample ultrastructure was examined under a JEM-1010 (JEOL) TEM (60 000 kV).

Additional experimental data are provided in Figure S5 (Supporting Information).

Supporting Information

Supporting Information is available from the Wiley Online Library or from the author.

Acknowledgements

M.G. and M.P.C. contributed equally to this work. The authors thank L Pedicini for support with the MNP synthesis. This work was partially supported by the Italian Miur (PRA 2016), the European Commission (MARVENE, NanosciE+ and MECAR 622122), and Fondazione Arpa. G.F.G. and M.P.C. are grateful for financial support from the DGA (Gobierno de Aragon, Project E26) and Spanish Ministerio de Economia y Competi-

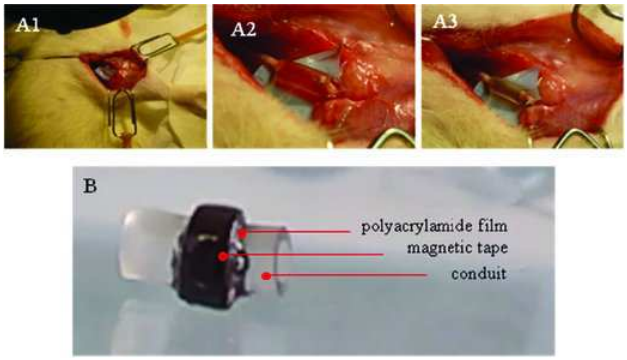

Figure 5. A) Surgical procedure. A1) The median nerve of an adult rat was cut (5 mm gap), and A2) a silicon tube was sutured between the two nerve stumps. A3) MNPs were injected in the tube. The liquid instantaneously filled the whole tube due to capillary force (the tube appears brown after MNP injection). B) Regeneration experiments: the conduit was wrapped with magnetic tape, and the tape was coated with a thin film of polyacrylamide.

tividad (MINECO) through project MAT2013-42551. M.G. was supported by a fellowship from Collegio Ghislieri, Pavia (Italy) and Fondazione Umberto Veronesi (Milano, Italy). V.R. was supported by a fellowship from the Marie Curie Programme.

Received: December 14, 2016
Published Online: MM DD, YYYY

[1] W. Daly, L. Yao, D. Zeugolis, A. Windebank, A. Pandit, *J. R. Soc., Interface* **2012**, *9*, 202.
[2] A. Piotrowicz, M. S. Shoichet, *Biomaterials* **2006**, *27*, 2018.
[3] B. J. Dickson, *Science* **2002**, *298*, 1959.
[4] M. Jubran, J. Widenfalk, *Exp. Neurol.* **2003**, *181*, 204.
[5] a) S. C. Apfel, *Am. J. Med.* **1999**, *107*, 34S; b) A. I. Gravvanis, D. A. Tsoutsos, G. A. Tagaris, A. E. Papalois, C. G. Patralexis, T. G. Iconomou, P. N. Panayotou, J. D. Ioannovich, *Microsurgery* **2004**, *24*, 408; c) E. G. Fine, I. Decosterd, M. Papaloizos, A. D. Zurn, P. Aebischer, *Eur. J. Neurosci.* **2002**, *15*, 589.
[6] W. Sun, C. Sun, H. Zhao, H. Lin, Q. Han, J. Wang, H. Ma, B. Chen, Z. Xiao, J. Dai, *PLoS One* **2009**, *4*, e6180.
[7] P. F. Pradat, *Rev. Neurol.* **2003**, *159*, 147.
[8] H. Yu, J. Peng, Q. Guo, L. Zhang, Z. Li, B. Zhao, X. Sui, Y. Wang, W. Xu, S. Lu, *Microsurgery* **2009**, *29*, 330.
[9] a) A. C. Lee, V. M. Yu, J. B. Lowe 3rd, M. J. Brenner, D. A. Hunter, S. E. Mackinnon, S. E. Sakiyama-Elbert, *Exp. Neurol.* **2003**, *184*, 295; b) Q. Yan, Y. Yin, B. Li, *Biomed. Eng. Online* **2012**, *11*, 36.
[10] M. I. Hobson, C. J. Green, G. Terenghi, *J. Anat.* **2000**, *197*, 591.
[11] a) V. H. Guaiquil, Z. Pan, N. Karagianni, S. Fukuoka, G. Alegre, M. I. Rosenblatt, *Proc. Natl. Acad. Sci. USA* **2014**, *111*, 17272; b) F. R. P. Lopes, B. C. G. Lisboa, F. Frattini, F. M. Almeida, M. A. Tomaz, P. K. Matsumoto, F. Langone, S. Lora, P. A. Melo, R. Borojevic, S. W. Han, A. M. B. Martinez, *Neuropath. Appl. Neuro* **2011**, *37*, 600; c) R. Mohammadi, S. Ahsan, M. Masoumi, K. Amini, *Chin. J. Traumatol.* **2013**, *16*, 323.
[12] S. M. Eppler, D. L. Combs, T. D. Henry, J. J. Lopez, S. G. Ellis, J. H. Yi, B. H. Annex, E. R. McCluskey, T. F. Zioncheck, *Clin. Pharmacol. Ther.* **2002**, *72*, 20.
[13] J. Y. Lee, G. Giusti, P. F. Friedrich, A. T. Bishop, A. Y. Shin, *J. Reconstr. Microsurg.* **2016**, *32*, 183.
[14] T. Gordon, *Neurosurg. Focus* **2009**, *26*, E3.
[15] S. Zhang, H. Uludag, *Pharm. Res.* **2009**, *26*, 1561.
[16] O. Ziv-Polat, A. Shahar, I. Levy, H. Skaat, S. Neuman, F. Fregnan, S. Geuna, C. Grothe, K. Haastert-Talini, S. Margel, *BioMed Res. Int.* **2014**, *2014*, 267808.
[17] H. Yu, J. Peng, Q. Guo, L. Zhang, Z. Li, B. Zhao, X. Sui, Y. Wang, W. Xu, S. Lu, *Microsurgery* **2009**, *29*, 330.
[18] M. I. Hobson, C. J. Green, G. Terenghi, *J. Anat.* **2000**, *197*, 591.
[19] C. E. Schmidt, J. B. Leach, *Ann. Rev. Biomed. Eng.* **2003**, *5*, 293.
[20] L. R. Williams, F. M. Longo, H. C. Powell, G. Lundborg, S. Varon, *J. Comp. Neurol.* **1983**, *218*, 460.
[21] J. S. Belkas, M. S. Shoichet, R. Midha, *Neurol. Res.* **2004**, *26*, 151.
[22] L. Diazflores, R. Gutierrez, H. Varela, P. Evora, F. Valladares, M. Rodriguez, N. Rancel, H. Alvarezarguelles, *Histol. Histopathol.* **1995**, *10*, 937.
[23] J. M. Pean, M. C. Venier-Julienne, F. Boury, P. Menei, B. Denizot, J. P. Benoit, *J. Controlled Release* **1998**, *56*, 175.
[24] M. Marcus, H. Skaat, N. Alon, S. Margel, O. Shefi, *Nanoscale* **2015**, *7*, 1058.
[25] C. Riggio, M. P. Calatayud, M. Giannaccini, B. Sanz, T. E. Torres, R. Fernandez-Pacheco, A. Ripoli, M. R. Ibarra, L. Dente, A. Cuschieri, G. F. Goya, V. Raffa, *Nanomed. Nanotechnol.* **2014**, *10*, 1549.
[26] K. Ulbrich, K. Hola, V. Subr, A. Bakandritsos, J. Tucek, R. Zboril, *Chem. Rev.* **2016**, *116*, 5338.
[27] M. P. Calatayud, C. Riggio, V. Raffa, B. Sanz, T. E. Torres, M. R. Ibarra, C. Hoskins, A. Cuschieri, L. Wang, J. Pinkernelle, G. Keilhofff, G. F. Goya, *J. Mater. Chem. B* **2013**, *1*, 3607.
[28] J. Pinkernelle, P. Calatayud, G. F. Goya, H. Fansa, G. Keilhoff, *BMC Neurosci.* **2012**, *13*, 32.
[29] J. Pinkernelle, V. Raffa, M. P. Calatayud, G. F. Goya, C. Riggio, G. Keilhoff, *Front. Neurosci.* **2015**, *9*, 305. Q7
[30] C. Riggio, S. Nocentini, M. P. Catalayud, G. F. Goya, A. Cuschieri, V. Raffa, J. A. del Rio, *Int. J. Mol. Sci.* **2013**, *14*, 10852.
[31] C. Riggio, M. P. Calatayud, C. Hoskins, J. Pinkernelle, B. Sanz, T. E. Torres, M. R. Ibarra, L. J. Wang, G. Keilhoff, G. F. Goya, V. Raffa, A. Cuschieri, *Int. J. Nanomed.* **2012**, *7*, 3155.
[32] J. A. Bertelli, M. Taleb, A. Saadi, J.-C. Mira, M. Pecot-Dechavassine, *Microsurgery* **1995**, *16*, 77.
[33] G. Ronchi, S. Nicolino, S. Raimondo, P. Tos, B. Battiston, I. Papalia, A. S. P. Varejão, M. G. Giacobini-Robecchi, I. Perroteau, S. Geuna, *J. Neurosci. Methods* **2009**, *179*, 51.
[34] J. A. Bertelli, J. C. Mira, *J. Neurosci. Methods* **1995**, *58*, 151. Q8
[35] L. J. Chamberlain, I. V. Yannas, H. P. Hsu, M. Spector, *J. Comp. Neurol.* **2000**, *417*, 415.
[36] G. N. Serbedzija, E. Flynn, C. E. Willett, *Angiogenesis* **1999**, *3*, 353.
[37] J. P. Smith, P. S. Hicks, L. R. Ortiz, M. J. Martinez, R. N. Mandler, *J. Neurosci. Methods* **1995**, *62*, 15.
[38] I. Papalia, P. Tos, F. S. d'Alcontres, B. Battiston, S. Geuna, *J. Neurosci. Methods* **2003**, *127*, 43.
[39] a) J. A. Bertelli, A. R. dos Santos, M. Taleb, J. B. Calixto, J. C. Mira, M. F. Ghizoni, *J. Neurosci. Methods* **2004**, *134*, 75; b) N. Sinis, H. E. Schaller, S. T. Becker, T. Lanaras, C. Schulte-Eversum, H. W. Muller, R. Vonthein, H. Rosner, M. Haerle, *J. Neurosci. Methods* **2006**, *156*, 166.

[40] M. Westerfield, *The Zebrafish Book: A Guide for the Laboratory Use of Zebrafish (Danio rerio)*, University of Oregon Press, Eugene **2007**.

Q1 APT to AU: Please provide Abstract (maximum of 200 words) for this paper. All abbreviations should be defined.
Q2 APT to AU: Please spell out the full first name for the author 'M. Pilar Calatayud' in the byline.
Q3 APT to AU: Please check presentation of Affiliation 5.
Q4 APT to AU: Please provide the highest academic title (Dr./Prof.) for all authors, where applicable.
Q5 APT to AU: The Author contributions statement has been set under Acknowledgements Section. Please check.
Q6 APT to AU: Please provide the expansion of HIV, FBS, DAB, ANOVA, BCIP and NBT as these have been cited once in the article.
Q7 APT to AU: Please check journal name in ref. (29).
Q8 APT to AU: The citations for refs. (34-40) are missing in the main text. Please cite references in the numerical order in the text.